

ANALYSIS OF PATCH SUBSTRUCTURING METHODS

MARTIN J. GANDER *, LAURENCE HALPERN **, FRÉDÉRIC MAGOULÈS ***,
FRANÇOIS-XAVIER ROUX ****

* Section de Mathématiques, Université de Genève
1211 Genève, Switzerland
e-mail: martin.gander@math.unige.ch

** LAGA, Institut Galilée, Université Paris 13
93430 Villetaneuse, France
e-mail: halpern@math.univ-paris13.fr

*** Applied Mathematics and Systems Laboratory, Ecole Centrale Paris
92295 Châtenay-Malabry Cedex, France
e-mail: frederic.magoules@hotmail.com

**** High Performance Computing Research Unit
ONERA, 92322 Chatillon, France
e-mail: roux@onera.fr

Patch substructuring methods are non-overlapping domain decomposition methods like classical substructuring methods, but they use information from geometric patches reaching into neighboring subdomains, condensed on the interfaces, to enhance the performance of the method, while keeping it non-overlapping. These methods are very convenient to use in practice, but their convergence properties have not been studied yet. We analyze geometric patch substructuring methods for the special case of one patch per interface. We show that this method is equivalent to an overlapping Schwarz method using Neumann transmission conditions. This equivalence is obtained by first studying a new, algebraic patch method, which is equivalent to the classical Schwarz method with Dirichlet transmission conditions and an overlap corresponding to the size of the patches. Our results motivate a new method, the Robin patch method, which is a linear combination of the algebraic and the geometric one, and can be interpreted as an optimized Schwarz method with Robin transmission conditions. This new method has a significantly faster convergence rate than both the algebraic and the geometric one. We complement our results by numerical experiments.

Keywords: Schwarz domain decomposition methods, Schur complement methods, patch substructuring methods, optimized Schwarz methods

1. Introduction

Substructuring methods are historically non-overlapping domain decomposition methods (Le Tallec, 1994; Quarteroni and Valli, 1999; Smith *et al.*, 1996; Toselli and Widlund, 2004). Patch substructuring methods are also non-overlapping domain decomposition methods, but they use information from within neighboring subdomains through geometric patches reaching into the neighboring subdomains, before being condensed algebraically onto the interfaces to obtain a non-overlapping method.

The idea of patch substructuring methods has its roots in the theory of optimized Schwarz methods, which

were developed at the continuous level in (Japhet, 1998) for advection diffusion problems, and in (Chevalier and Nataf, 1998) for Helmholtz problems, based on the non-overlapping method first introduced in (Lions, 1990). These methods use as transmission conditions approximations of the Steklov-Poincaré operator at the interfaces between subdomains, which greatly enhances their performance. For a complete review of the historical development of these methods, and results for symmetric positive definite problems, see (Gander, 2006). Patch substructuring methods are the discrete analog of optimized Schwarz methods: they use approximations of the Schur comple-

ment condensated on the interfaces between subdomains to enhance the performance of the method. If the entire Schur complement is used, optimal iteration numbers can be achieved like at the continuous level with the Steklov-Poincaré operator, see (Magoulès *et al.*, 2004b). Approximations are, however, obtained differently, namely, by computing approximate Schur complements based on patches. We call this original patch method the geometric patch method, since it uses the underlying finite element mesh to define the patches. So far, convergence properties of patch substructuring methods have not been studied, but numerical experiments in (Magoulès *et al.*, 2005; Magoulès *et al.*, 2006) showed that the addition of these patches significantly enhances the performance of the domain decomposition method, and is easily achieved in practice, provided the geometry of the discretization is known.

In this paper we show that a particular case of the geometric patch method, namely, the case of one patch per subdomain interface leads to an algorithm equivalent to an overlapping Schwarz method with Neumann transmission conditions at the new interface locations defined by the end of the patches. This equivalence is obtained by first studying a new patch method, which we call the algebraic patch method, which is equivalent to the classical Schwarz method with Dirichlet transmission conditions, see (Lions, 1988; Schwarz, 1870). Algebraic patch methods can be constructed without geometric information from the underlying mesh, directly based on the matrix, and their convergence depends on the size of the patches, which represents the overlap of the equivalent classical Schwarz method, see, e.g., (Smith *et al.*, 1996). Hence algebraic patch substructuring methods converge independently of the mesh parameter if the patch size is constant in physical space. The same seems to be true for the geometric patch method, as indicated by the numerical results in this paper. While one can prove this for simple model problems by Fourier analysis, to our knowledge currently there is no convergence theory for Schwarz methods with Neumann transmission conditions.

Our results motivate a new, third patch method, namely, a linear combination of the algebraic and the geometric one, which we call the Robin patch method. It can be interpreted as an optimized Schwarz method with Robin transmission conditions at the end of the patch, which, following the developments of optimized Schwarz methods, yields significantly faster convergence rates than both the algebraic and geometric patch methods.

This paper is organized as follows: In Section 2, we present the decomposition of a model problem into subproblems, and show the equivalence of the decomposed problem and the original one. In Section 3, we present an entire family of substructuring methods, and show that an optimal algorithm would need to involve Schur complements. In Section 4, we present the geometric and al-

gebraic patch methods, and analyze the particular case of one patch per subdomain interface by showing its equivalence to Schwarz domain decomposition methods. We also introduce the new idea of Robin patch methods. We show numerical experiments in Section 5 which confirm our analysis, and also indicate the great potential of the new Robin patch method. We conclude in Section 6 with a summary and a discussion of open problems.

2. Domain Decomposition

To fix ideas, we consider the model problem

$$\mathcal{L}(u) = f \quad \text{in } \Omega \subset \mathbb{R}^2, \tag{1}$$

where \mathcal{L} is a second-order elliptic operator. We assume that this problem is completed with suitable boundary conditions which lead to a well-posed problem. Discretizing (1) by a finite element or finite difference method leads to the discrete problem

$$Ku = f, \tag{2}$$

where K is the stiffness matrix, u is the discrete approximation of the solution u , and f is the discrete approximation of the right-hand side f .

To keep the notation simple, and without loss of generality, we decompose the domain Ω into two non-overlapping subdomains Ω_1 and Ω_2 only, as shown in Fig. 1. At the discrete level this decomposition leads to

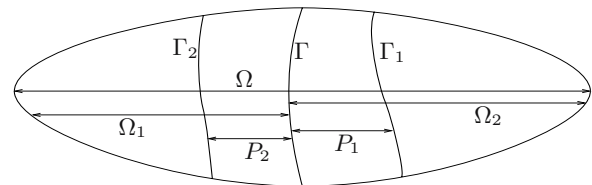


Fig. 1. Non-overlapping domain decomposition, with patches P_1 and P_2 .

the matrix partitioning

$$\begin{pmatrix} K_1 & K_{1\Gamma} \\ K_{\Gamma 1} & K_\Gamma & K_{\Gamma 2} \\ & K_{2\Gamma} & K_2 \end{pmatrix} \begin{pmatrix} u_1 \\ u_\Gamma \\ u_2 \end{pmatrix} = \begin{pmatrix} f_1 \\ f_\Gamma \\ f_2 \end{pmatrix}, \tag{3}$$

where u_Γ corresponds to the unknowns on the interface Γ , and $u_j, j = 1, 2$ represent the unknowns in the interior of the non-overlapping subdomains Ω_1 and Ω_2 . In a finite element discretization, it is natural to split the interface matrix K_Γ into two parts, $K_\Gamma = K_\Gamma^1 + K_\Gamma^2$, where K_Γ^1 represents the contribution of the elements to the left of the interface Γ , and K_Γ^2 the contribution of the elements to the right of the interface Γ . Similarly, also the right-hand side vector on the interface can naturally be split into two parts, $f_\Gamma = f_\Gamma^1 + f_\Gamma^2$. For discretizations other than finite

elements, such a splitting is less natural, but other splittings could be used, as we will see later. The following theorem shows the equivalence of an entire class of decomposed problems to the underlying original problem, see (Magoulès *et al.*, 2004b):

Theorem 1. *For any splitting of the form $K_\Gamma = K_\Gamma^1 + K_\Gamma^2$ and $\mathbf{f}_\Gamma = \mathbf{f}_\Gamma^1 + \mathbf{f}_\Gamma^2$, and for all matrices A_1 and A_2 of size of the matrix K_Γ , there is one and only one λ_1, λ_2 such that the decoupled problems*

$$\begin{pmatrix} K_1 & K_{1\Gamma} \\ K_{\Gamma 1} & K_\Gamma^1 + A_1 \end{pmatrix} \begin{pmatrix} \mathbf{u}_1 \\ \mathbf{u}_{\Gamma 1} \end{pmatrix} = \begin{pmatrix} \mathbf{f}_1 \\ \mathbf{f}_{\Gamma 1} + \lambda_1 \end{pmatrix}, \quad (4)$$

$$\begin{pmatrix} K_\Gamma^2 + A_2 & K_{\Gamma 2} \\ K_{2\Gamma} & K_2 \end{pmatrix} \begin{pmatrix} \mathbf{u}_{\Gamma 2} \\ \mathbf{u}_2 \end{pmatrix} = \begin{pmatrix} \mathbf{f}_{\Gamma 2} + \lambda_2 \\ \mathbf{f}_2 \end{pmatrix}, \quad (5)$$

together with the coupling conditions

$$\begin{aligned} \mathbf{u}_{\Gamma 1} - \mathbf{u}_{\Gamma 2} &= 0, \\ \lambda_1 + \lambda_2 - A_1 \mathbf{u}_{\Gamma 1} - A_2 \mathbf{u}_{\Gamma 2} &= 0, \end{aligned} \quad (6)$$

are equivalent to the original problem (3) with $\mathbf{u}_\Gamma = \mathbf{u}_{\Gamma 1} = \mathbf{u}_{\Gamma 2}$.

Proof. If $\mathbf{u}_1, \mathbf{u}_2$ and \mathbf{u}_Γ constitute a solution of (3), then with $\mathbf{u}_{\Gamma 1} := \mathbf{u}_\Gamma, \mathbf{u}_{\Gamma 2} := \mathbf{u}_\Gamma$ and

$$\begin{aligned} \lambda_1 &:= K_{\Gamma 1} \mathbf{u}_1 + (K_\Gamma^1 + A_1) \mathbf{u}_\Gamma - \mathbf{f}_{\Gamma 1}, \\ \lambda_2 &:= K_{\Gamma 2} \mathbf{u}_2 + (K_\Gamma^2 + A_2) \mathbf{u}_\Gamma - \mathbf{f}_{\Gamma 2}. \end{aligned}$$

Equations (4) and (5) are satisfied, together with the coupling conditions (6).

Conversely, if $\mathbf{u}_1, \mathbf{u}_2, \mathbf{u}_{\Gamma 1}$ and $\mathbf{u}_{\Gamma 2}$ form a solution of (4) and (5), where λ_1 and λ_2 satisfy the coupling conditions (6), then with $\mathbf{u}_\Gamma := \mathbf{u}_{\Gamma 1} (= \mathbf{u}_{\Gamma 2})$, adding the second equation of (4) and the first equation of (5) shows that $\mathbf{u}_1, \mathbf{u}_2$ and \mathbf{u}_Γ is solution of (3). ■

3. Family of Substructuring Methods and an Optimal One

The decoupled problems (4) and (5) together with the coupling conditions (6) lead naturally to an iterative substructuring algorithm: starting with approximations λ_1^0 and λ_2^0 , it computes for $k = 0, 1, 2, \dots$ iteratively the updates

$$\begin{pmatrix} K_1 & K_{1\Gamma} \\ K_{\Gamma 1} & K_\Gamma^1 + A_1 \end{pmatrix} \begin{pmatrix} \mathbf{u}_1^k \\ \mathbf{u}_{\Gamma 1}^k \end{pmatrix} = \begin{pmatrix} \mathbf{f}_1 \\ \mathbf{f}_{\Gamma 1} + \lambda_1^k \end{pmatrix}, \quad (7)$$

$$\begin{pmatrix} K_\Gamma^2 + A_2 & K_{\Gamma 2} \\ K_{2\Gamma} & K_2 \end{pmatrix} \begin{pmatrix} \mathbf{u}_{\Gamma 2}^k \\ \mathbf{u}_2^k \end{pmatrix} = \begin{pmatrix} \mathbf{f}_{\Gamma 2} + \lambda_2^k \\ \mathbf{f}_2 \end{pmatrix}, \quad (8)$$

$$\lambda_1^{k+1} = -\lambda_2^k + (A_1 + A_2) \mathbf{u}_{\Gamma 2}^k, \quad (9)$$

$$\lambda_2^{k+1} = -\lambda_1^k + (A_1 + A_2) \mathbf{u}_{\Gamma 1}^k. \quad (10)$$

In order for the transmission conditions (9) and (10) to imply the coupling conditions (6) at convergence, we need to impose that the sum $A_1 + A_2$ is invertible. To gain more insight into the algorithm (7)–(10), we eliminate λ_j^k from the right-hand side of the updates for λ_j^{k+1} by using the subdomain equations containing λ_j^k . This gives at step k the new updates

$$\lambda_1^k = \mathbf{f}_{\Gamma 2} - K_{\Gamma 2} \mathbf{u}_2^{k-1} + (A_1 - K_\Gamma^2) \mathbf{u}_{\Gamma 2}^{k-1}, \quad (11)$$

$$\lambda_2^k = \mathbf{f}_{\Gamma 1} - K_{\Gamma 1} \mathbf{u}_1^{k-1} + (A_2 - K_\Gamma^1) \mathbf{u}_{\Gamma 1}^{k-1}. \quad (12)$$

Inserting these values into the subdomain equations in (7) and (8), we obtain an equivalent algorithm, which is now independent of λ_1^k and λ_2^k , namely,

$$\begin{pmatrix} K_1 & K_{1\Gamma} \\ K_{\Gamma 1} & K_\Gamma^1 + A_1 \end{pmatrix} \begin{pmatrix} \mathbf{u}_1^k \\ \mathbf{u}_{\Gamma 1}^k \end{pmatrix} = \begin{pmatrix} \mathbf{f}_1 \\ \mathbf{f}_{\Gamma 1} - K_{\Gamma 2} \mathbf{u}_2^{k-1} + (A_1 - K_\Gamma^2) \mathbf{u}_{\Gamma 2}^{k-1} \end{pmatrix}, \quad (13)$$

$$\begin{pmatrix} K_\Gamma^2 + A_2 & K_{\Gamma 2} \\ K_{2\Gamma} & K_2 \end{pmatrix} \begin{pmatrix} \mathbf{u}_{\Gamma 2}^k \\ \mathbf{u}_2^k \end{pmatrix} = \begin{pmatrix} \mathbf{f}_{\Gamma 2} - K_{\Gamma 1} \mathbf{u}_1^{k-1} + (A_2 - K_\Gamma^1) \mathbf{u}_{\Gamma 1}^{k-1} \\ \mathbf{f}_2 \end{pmatrix}. \quad (14)$$

The performance of the substructuring algorithm (7)–(10) (or, equivalently, the algorithm (13), (14)) is strongly influenced by the choice of the matrices A_1 and A_2 . A simple choice is $A_1 = K_\Gamma^2$ and $A_2 = K_\Gamma^1$, which, when inserted into (13) and (14), shows that this is equivalent to the classical Schwarz method with two mesh sizes overlap. The optimal choice for our case is given by the following theorem:

Theorem 2. *If $A_1 = K_\Gamma^2 - K_{\Gamma 2} K_2^{-1} K_{2\Gamma}$, and $A_2 = K_\Gamma^1 - K_{\Gamma 1} K_1^{-1} K_{1\Gamma}$, then the algorithm (13)–(14) converges in two iterations for any initial guess $\mathbf{u}_1^0, \mathbf{u}_{\Gamma 1}^0, \mathbf{u}_2^0, \mathbf{u}_{\Gamma 2}^0$.*

Proof. We show the result for the first subproblem since the argument for the second is similar. At iteration $k = 1$, by multiplying the second equation in (14) by $K_{\Gamma 2} K_2^{-1}$ we obtain the relation

$$K_{\Gamma 2} \mathbf{u}_2^1 + K_{\Gamma 2} K_2^{-1} K_{2\Gamma} \mathbf{u}_{\Gamma 2}^1 = K_{\Gamma 2} K_2^{-1} \mathbf{f}_2,$$

which leads at iteration $k = 2$ together with the definition of A_1 to the first subdomain problem

$$\begin{pmatrix} K_1 & K_{1\Gamma} \\ K_{\Gamma 1} & K_\Gamma - K_{\Gamma 2} K_2^{-1} K_{2\Gamma} \end{pmatrix} \begin{pmatrix} \mathbf{u}_1^2 \\ \mathbf{u}_{\Gamma 1}^2 \end{pmatrix} = \begin{pmatrix} \mathbf{f}_1 \\ \mathbf{f}_{\Gamma 1} - K_{\Gamma 2} K_2^{-1} \mathbf{f}_2 \end{pmatrix}.$$

This is, however, nothing else than a system equivalent to the original undecomposed problem (3), where the variables u_2 have been eliminated using the Schur complement. Therefore $u_1^2 = u_1$ and $u_{\Gamma_1}^2 = u_{\Gamma}$. ■

4. Patch Substructuring Methods

In (Magoulès et al., 2004b; Magoulès et al., 2005; Magoulès et al., 2006), it was proposed to approximate the optimal choice of A_1 and A_2 , which is based on the Schur complement of the entire neighboring subdomain, by a Schur complement on patches reaching from the interface Γ into the neighboring subdomain. We use here one patch per subdomain interface, denoted by P_1 and P_2 , with external boundaries Γ_1 and Γ_2 , see Fig. 1. To reflect these patches in the discretized problem, we rewrite the global system (2) in the more detailed form

$$\begin{pmatrix} K_1 & K_{1\Gamma_2} \\ K_{\Gamma_2 1} & K_{\Gamma_2} & K_{\Gamma_2 P_2} \\ & K_{P_2 \Gamma_2} & K_{P_2} & K_{P_2 \Gamma} \\ & & K_{\Gamma P_2} & K_{\Gamma} & K_{\Gamma P_1} \\ & & & K_{P_1 \Gamma} & K_{P_1} & K_{P_1 \Gamma_1} \\ & & & & K_{\Gamma_1 P_1} & K_{\Gamma_1} & K_{\Gamma_1 2} \\ & & & & & K_{2\Gamma_1} & K_2 \end{pmatrix} \begin{pmatrix} u_1 \\ u_{\Gamma_2} \\ u_{P_2} \\ u_{\Gamma} \\ u_{P_1} \\ u_{\Gamma_1} \\ u_2 \end{pmatrix} = \begin{pmatrix} f_1 \\ f_{\Gamma_2} \\ f_{P_2} \\ f_{\Gamma} \\ f_{P_1} \\ f_{\Gamma_1} \\ f_2 \end{pmatrix}. \tag{15}$$

Note that we reused the symbols K_j , which represent now the discretization matrix for the partial subdomains $\Omega_i - P_j, i \neq j$, and similarly for the vectors u_j and $f_j, j = 1, 2$.

In a simple patch method, the optimal choice of A_1 and A_2 in Theorem 2 is approximated by

$$A_1 = K_{\Gamma}^2 - (K_{\Gamma P_1} \ 0) \begin{pmatrix} K_{P_1} & K_{P_1 \Gamma_1} \\ K_{\Gamma_1 P_1} & K_{\Gamma_1}^1 \end{pmatrix}^{-1} \begin{pmatrix} K_{P_1 \Gamma} \\ 0 \end{pmatrix}, \tag{16}$$

$$A_2 = K_{\Gamma}^1 - (0 \ K_{\Gamma P_2}) \begin{pmatrix} K_{\Gamma_2}^2 & K_{\Gamma_2 P_2} \\ K_{P_2 \Gamma_2} & K_{P_2} \end{pmatrix}^{-1} \begin{pmatrix} 0 \\ K_{P_2 \Gamma} \end{pmatrix}. \tag{17}$$

In the geometric patch approach, the natural splittings $K_{\Gamma_1} = K_{\Gamma_1}^1 + K_{\Gamma_1}^2$ and $K_{\Gamma_2} = K_{\Gamma_2}^1 + K_{\Gamma_2}^2$, induced by the finite element contribution to the left and right of the patch boundaries Γ_1 and Γ_2 , respectively, are used to

define $K_{\Gamma_1}^1$ and $K_{\Gamma_2}^2$, and thus knowledge of the geometry of the problem is required. In the algebraic approach, we propose to set $K_{\Gamma_1}^1 := K_{\Gamma_1}$ and $K_{\Gamma_2}^2 := K_{\Gamma_2}$, which can be performed directly at the matrix level.

We now show that the algebraic patch method corresponds to a classical Schwarz method with an overlap of the size of the patches. A classical Schwarz method with Dirichlet transmission conditions and subdomains Ω_j enlarged by the patches $P_j, j = 1, 2$, is given by the iteration

$$\begin{pmatrix} K_1 & K_{1\Gamma_2} \\ K_{\Gamma_2 1} & K_{\Gamma_2} & K_{\Gamma_2 P_2} \\ & K_{P_2 \Gamma_2} & K_{P_2} & K_{P_2 \Gamma} \\ & & K_{\Gamma P_2} & K_{\Gamma} & K_{\Gamma P_1} \\ & & & K_{P_1 \Gamma} & K_{P_1} & K_{P_1 \Gamma_1} \\ & & & & K_{\Gamma_1 P_1} & K_{\Gamma_1} \end{pmatrix} \begin{pmatrix} v_1^k \\ v_{\Gamma_2}^k \\ v_{P_2}^k \\ v_{\Gamma}^k \\ v_{P_1}^k \\ v_{\Gamma_1}^k \end{pmatrix} = \begin{pmatrix} f_1 \\ f_{\Gamma_2} \\ f_{P_2} \\ f_{\Gamma} \\ f_{P_1} \\ f_{\Gamma_1} - K_{\Gamma_1 2} w_2^{k-1} \end{pmatrix}, \tag{18}$$

$$\begin{pmatrix} K_{\Gamma_2} & K_{\Gamma_2 P_2} \\ K_{P_2 \Gamma_2} & K_{P_2} & K_{P_2 \Gamma} \\ & K_{\Gamma P_2} & K_{\Gamma} & K_{\Gamma P_1} \\ & & K_{P_1 \Gamma} & K_{P_1} & K_{P_1 \Gamma_1} \\ & & & K_{\Gamma_1 P_1} & K_{\Gamma_1} & K_{\Gamma_1 2} \\ & & & & K_{2\Gamma_1} & K_2 \end{pmatrix} \begin{pmatrix} w_{\Gamma_2}^k \\ w_{P_2}^k \\ w_{\Gamma}^k \\ w_{P_1}^k \\ w_{\Gamma_1}^k \\ w_2^k \end{pmatrix} = \begin{pmatrix} f_{\Gamma_2} - K_{\Gamma_2 1} v_1^{k-1} \\ f_{P_2} \\ f_{\Gamma} \\ f_{P_1} \\ f_{\Gamma_1} \\ f_2 \end{pmatrix}, \tag{19}$$

where we used v and w to distinguish the Schwarz iterates from the iterates of the patch method.

Theorem 3. The classical Schwarz method (18)–(19) and the substructuring method (7)–(10) with the algebraic patches (16)–(17) produce for $k = 2, 3, \dots$ the same sequence of iterates

$$\begin{pmatrix} v_1^k \\ v_{\Gamma_2}^k \\ v_{P_2}^k \\ v_{\Gamma}^k \end{pmatrix} = \begin{pmatrix} u_1^k \\ u_{\Gamma_1}^k \end{pmatrix}, \quad \begin{pmatrix} w_{\Gamma}^k \\ w_{P_1}^k \\ w_{\Gamma_1}^k \\ w_2^k \end{pmatrix} = \begin{pmatrix} u_{\Gamma_2}^k \\ u_2^k \end{pmatrix},$$

provided that

$$\begin{pmatrix} \mathbf{v}_\Gamma^1 \\ \mathbf{v}_{\Gamma_2}^1 \\ \mathbf{v}_{P_2}^1 \\ \mathbf{v}_\Gamma^1 \end{pmatrix} = \begin{pmatrix} \mathbf{u}_1^1 \\ \mathbf{u}_{\Gamma_1}^1 \end{pmatrix}, \quad \begin{pmatrix} \mathbf{w}_\Gamma^1 \\ \mathbf{w}_{P_1}^1 \\ \mathbf{w}_{\Gamma_1}^1 \\ \mathbf{w}_2^1 \end{pmatrix} = \begin{pmatrix} \mathbf{u}_{\Gamma_2}^1 \\ \mathbf{u}_2^1 \end{pmatrix}.$$

Proof. The proof is by induction. For $k = 1$, the result holds by assumption. To show the result for $k > 1$, it suffices to show that the subdomain problems in each iteration coincide. To this end, we eliminate in Subdomain 1 of the classical Schwarz method (18)–(19) (and, similarly, in Subdomain 2) the unknowns $\mathbf{v}_{P_1}^k$ and $\mathbf{v}_{\Gamma_1}^k$. From the subdomain equations, we obtain

$$\begin{pmatrix} \mathbf{v}_{P_1}^k \\ \mathbf{v}_{\Gamma_1}^k \end{pmatrix} = \begin{pmatrix} K_{P_1} & K_{P_1\Gamma_1} \\ K_{\Gamma_1 P_1} & K_{\Gamma_1}^1 \end{pmatrix}^{-1} \begin{pmatrix} \mathbf{f}_{P_1} - K_{P_1\Gamma} \mathbf{v}_\Gamma^k \\ \mathbf{f}_{\Gamma_1} - K_{\Gamma_1 2} \mathbf{w}_2^{k-1} \end{pmatrix},$$

which implies

$$\begin{aligned} & K_{\Gamma P_1} \mathbf{v}_{P_1}^k \\ &= -(K_{\Gamma P_1} \ 0) \begin{pmatrix} K_{P_1} & K_{P_1\Gamma_1} \\ K_{\Gamma_1 P_1} & K_{\Gamma_1}^1 \end{pmatrix}^{-1} \begin{pmatrix} K_{P_1\Gamma} \\ 0 \end{pmatrix} \mathbf{v}_\Gamma^k \\ &+ (K_{\Gamma P_1} \ 0) \begin{pmatrix} K_{P_1} & K_{P_1\Gamma_1} \\ K_{\Gamma_1 P_1} & K_{\Gamma_1}^1 \end{pmatrix}^{-1} \begin{pmatrix} \mathbf{f}_{P_1} \\ \mathbf{f}_{\Gamma_1} - K_{\Gamma_1 2} \mathbf{w}_2^{k-1} \end{pmatrix}, \end{aligned}$$

where we recognize in the first term on the right of the equals sign the second part of the patch operator A_1 given in (16) and (17). The first subdomain equation can therefore be written in the equivalent form

$$\begin{pmatrix} K_1 & K_{1\Gamma_2} \\ K_{\Gamma_2 1} & K_{\Gamma_2} & K_{\Gamma_2 P_2} \\ & K_{P_2 \Gamma_2} & K_{P_2} & K_{P_2 \Gamma} \\ & & K_{\Gamma P_2} & K_\Gamma + A_1 - K_\Gamma^2 \end{pmatrix} \begin{pmatrix} \mathbf{v}_1^k \\ \mathbf{v}_{\Gamma_2}^k \\ \mathbf{v}_{P_2}^k \\ \mathbf{v}_\Gamma^k \end{pmatrix} = \begin{pmatrix} \mathbf{f}_1 \\ \mathbf{f}_{\Gamma_2} \\ \mathbf{f}_{P_2} \\ \mathbf{f}_\Gamma - (K_{\Gamma P_1} \ 0) \begin{pmatrix} K_{P_1} & K_{P_1\Gamma_1} \\ K_{\Gamma_1 P_1} & K_{\Gamma_1}^1 \end{pmatrix}^{-1} \begin{pmatrix} \mathbf{f}_{P_1} \\ \mathbf{f}_{\Gamma_1} - K_{\Gamma_1 2} \mathbf{w}_2^{k-1} \end{pmatrix} \end{pmatrix}. \tag{20}$$

Now, using the equations of the second subdomain at step $k - 1$, we find from

$$\begin{pmatrix} K_{P_1\Gamma} \\ 0 \end{pmatrix} \mathbf{w}_\Gamma^{k-1} + \begin{pmatrix} K_{P_1} & K_{P_1\Gamma_1} \\ K_{\Gamma_1 P_1} & K_{\Gamma_1}^1 \end{pmatrix} \begin{pmatrix} \mathbf{w}_{P_1}^{k-1} \\ \mathbf{w}_{\Gamma_1}^{k-1} \end{pmatrix} = \begin{pmatrix} \mathbf{f}_{P_1} \\ \mathbf{f}_{\Gamma_1} - K_{\Gamma_1 2} \mathbf{w}_2^{k-1} \end{pmatrix}$$

that the transmitted term on the right-hand side in (20) satisfies

$$\begin{aligned} & (K_{\Gamma P_1} \ 0) \begin{pmatrix} K_{P_1} & K_{P_1\Gamma_1} \\ K_{\Gamma_1 P_1} & K_{\Gamma_1}^1 \end{pmatrix}^{-1} \begin{pmatrix} \mathbf{f}_{P_1} \\ \mathbf{f}_{\Gamma_1} - K_{\Gamma_1 2} \mathbf{w}_2^{k-1} \end{pmatrix} \\ &= (K_\Gamma^2 - A_1) \mathbf{w}_\Gamma^{k-1} + K_{\Gamma P_1} \mathbf{w}_{P_1}^{k-1}. \end{aligned}$$

Inserting this into (20), the subdomain problem coincides with the subdomain problem of (13), which is equivalent to the patch method (7). A similar argument on the second subdomain concludes the proof. ■

Note that the same argument also holds in the case of the geometric patch, except that the subdomain problems now have Neumann (natural) conditions at the artificial boundaries between subdomains.

Instead of computing the Schur complement of the entire patch, one can also compute Schur complements of smaller parts of the patch and then add them to approximate the Schur complement of the entire patch, see (Magoulès *et al.*, 2004b; Magoulès *et al.*, 2005; Magoulès *et al.*, 2006). The present analysis does not apply to this case, and this additional approximation requires further studies.

The relation between patch substructuring methods and Schwarz methods allows us to determine a more effective patch, which is obtained by taking a linear combination of the algebraic and the geometric patch. While the interior of the patch remains unchanged, at the exterior boundary of the patch now a linear combination of Dirichlet and Neumann conditions is imposed, which results in a Robin condition, like in optimized Schwarz methods, see (Gander, 2006). Using a well-chosen linear combination will greatly enhance the convergence of the method, as we will see in the numerical experiments.

5. Numerical Experiments

In order to accelerate the convergence of the iterative method (7)–(10), one usually applies a Krylov method (Saad, 1996) to solve directly the interface system formulated in the variables λ_1 and λ_2 , see (Magoulès *et al.*, 2004a). This interface system is obtained by considering (7)–(10) without iteration index k , eliminating \mathbf{u}_1 and \mathbf{u}_2 from (7) and (8), and then inserting the resulting values for \mathbf{u}_{Γ_1} and \mathbf{u}_{Γ_2} into (9) and (10), which results in a system in the interface unknowns λ_1 and λ_2 only. The matrix of this interface system is a dense matrix and is not known explicitly, since it depends on subdomain quantities that have been used to eliminate \mathbf{u}_1 and \mathbf{u}_2 . Using a Krylov method on this interface system involves a matrix vector product by this matrix at each iteration, and hence subdomain solves. This is then the main part of the computation, but the local subproblems can be solved at each iteration

in parallel, one on each processor. The remainder of the computation consists of scalar products and linear combinations of vectors. From an implementation point of view, the product of a vector and the interface matrix needs only data that are local to each processor. This product is performed by first using the matrices of subproblems which are local to each processor and then assembling the result over all of the processors. The subdomain problems can be solved either by matrix factorization, or again by an iterative method, which then leads to inner-outer iteration methods.

We first present two numerical experiments to illustrate the convergence properties of the geometric patch method. We use directly a Krylov method on the corresponding interface system in this subsection, and the stopping criterion is set to 10^{-6} on the global residual.

The first problem consists of a two-dimensional beam of length $L = 10$ and height $l = 1$ submitted to flexion, as shown in Fig. 2. The Poisson ratio and

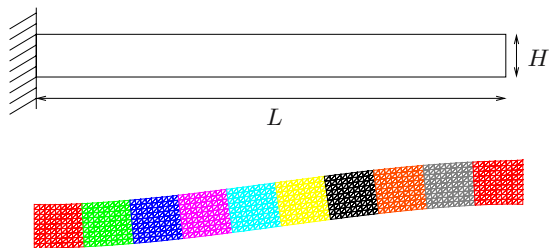


Fig. 2. Geometry (top) and displacement (bottom) of the cantilever beam.

the Young modulus are respectively $\nu = 0.3$ and $E = 2.0 \cdot 10^5 \text{ Nm}^{-2}$. Homogeneous Dirichlet boundary conditions are imposed on the left, and homogeneous Neumann boundary conditions are imposed on the top and at the bottom. Loading, modeled as nonhomogeneous Dirichlet boundary conditions, is imposed on the right of the structure. The beam is meshed with triangular elements and discretized with Lagrange finite elements involving two degrees of freedom per node. The mesh is then split into ten subdomains and the displacement is evaluated, see Fig. 2. The performance of the geometric patch algorithm is shown in Table 1, for both the case with a constant patch size in physical space and that with a patch size proportional to the mesh parameter. These results show that the number of iterations is constant for a fixed patch size in physical space, and grows if the patch size is proportional to the mesh size, as expected from the equivalence with Schwarz methods with Neumann transmission conditions.

In Table 2, we show iteration counts for the geometric patch method used with a constant mesh size h for different sizes of the patch. We see that increasing the patch size reduces the number of iterations, as expected from the equivalence with the Schwarz method.

Table 1. Number of iterations for different mesh sizes h , a patch proportional to h and a constant patch size for the cantilever beam problem (case of ten subdomains).

Mesh size h	Patch size	Number of iterations	Patch size	Number of iterations
1/10	$4h$	29	$2h$	40
1/20	$4h$	44	$4h$	44
1/40	$4h$	61	$8h$	46
1/80	$4h$	83	$16h$	47

Table 2. Number of iterations for a constant mesh size h , and different patch sizes for the cantilever beam problem (case of ten subdomains).

Mesh size h	Patch size	Number of iterations
1/40	$2h$	77
1/40	$4h$	61
1/40	$8h$	46
1/40	$16h$	33
1/40	$32h$	29

The second problem is the Scordelis-Lo roof problem. Here a cylindrical roof is loaded by its own weight, as shown in Fig. 3. The geometric characteristics are $R = 300$, $L = 1200$, and $H = 0.4$. The Poisson ratio ν and the Young modulus E are respectively $\nu = 0.3$ and $E = 2 \cdot 10^5 \text{ Nm}^{-2}$. Due to the symmetry of the geometry only one fourth of the roof is meshed. A finite element discretization with DKT (Discrete Kirchhoff Triangle) shell elements involving three nodes per element and six degrees of freedom per node is performed. The displacement of the roof is shown in Fig. 4. To compute this result, the mesh is split into four subdomains, and the geometric patch substructuring method is applied. The number of iterations required is shown in Table 3, where the size of the overlap is proportional to the mesh parameter.

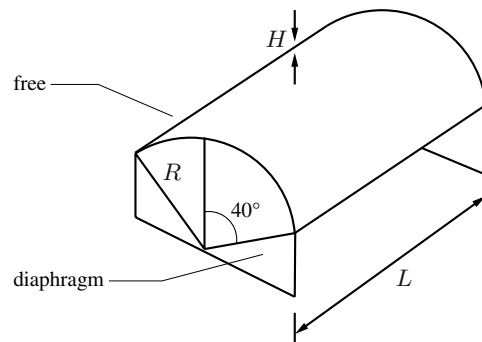


Fig. 3. Geometry of the Scordelis-Lo roof.

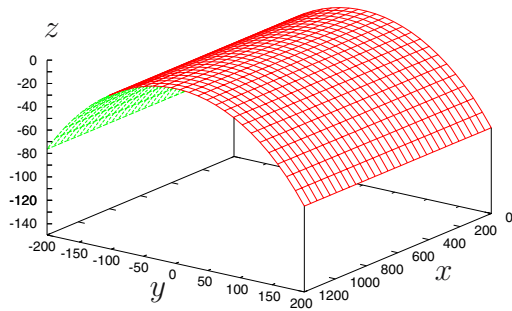


Fig. 4. Displacement of the Scordelis-Lo roof.

Table 3. Number of iterations for different mesh sizes h , for a patch proportional to h and a constant patch size for the Scordelis-Lo roof problem (case of four subdomains).

Mesh size h	Patch size	Number of iterations	Patch size	Number of iterations
1/100	$4h$	17	$2h$	36
1/200	$4h$	36	$4h$	36
1/400	$4h$	56	$8h$	36
1/800	$4h$	87	$16h$	38

We compare now the algebraic, geometric and Robin patch methods, of which the latter is a linear combination of the former two, on the model problem

$$(\eta - \Delta)u = f \quad \text{in } \Omega = (0, 1) \times (0, 1), \quad (21)$$

with homogeneous boundary conditions. We partition Ω into two subdomains $\Omega_1 = (0, \frac{1}{2}) \times (0, 1)$ and $\Omega_2 = (\frac{1}{2}, 1) \times (0, 1)$. We discretize the problem with the standard five point finite difference stencil on a uniform mesh with mesh parameter $h = 1/(n + 1)$, where n is the number of discretization points in both the x and y directions. Figure 5 shows the results we obtain by using the three different patch methods as iterative solvers and with Krylov acceleration for $\eta = 1$ and a patch size of $2h = 1/25$ with $h = 1/50$. We can see that the algebraic patch method converges a bit faster than the geometric patch method for this example, but these methods are comparable. Both are also greatly accelerated when used together with a Krylov method. Much faster, however, is the new Robin patch method, even without Krylov acceleration. In the Robin patch method, we used a linear combination based on the Robin parameter of optimized Schwarz methods, see (Gander, 2006).

In Table 4 we show the number of iterations needed to reduce the initial residual by a factor of 10^{-6} , when patch methods are used as iterative solvers, and the mesh is refined, both in the case of a fixed patch size, and a patch

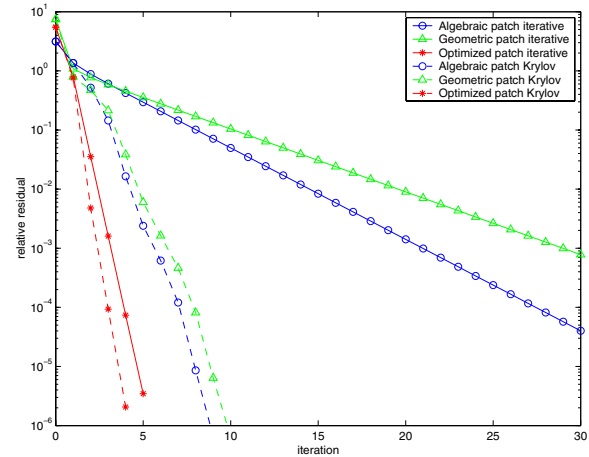


Fig. 5. Comparison of the algebraic, geometric and Robin patch methods for a model problem.

Table 4. Number of iterations for different mesh sizes h , for a patch proportional to h and a constant patch size for the model problem, when the method is used without Krylov acceleration.

Mesh size h	Patch size	Geometric	Algebraic	Robin
1/50	$2h$	39	57	5
1/100	$2h$	77	111	7
1/200	$2h$	154	224	8
1/400	$2h$	306	444	10
1/50	$4h$	39	57	5
1/100	$4h$	43	56	5
1/200	$8h$	46	56	5
1/400	$16h$	47	56	5

size proportional to h . If the patch size is proportional to h , the number of iterations increases when the mesh is refined, for all patch methods, but the increase is very moderate for the optimized patch method. For a fixed patch size, all patch methods are robust with respect to mesh refinement, but again by far the fastest is the Robin patch method.

In Table 5 we show the same sequence of experiments, but now using Krylov acceleration. All iteration numbers are now lower, in particular the ones for the algebraic and geometric patch methods.

We finally show for the case of a patch with the size dependent on h the iteration counts in a graph in Fig. 6. Here one can clearly see that the Robin patch method has a significant asymptotic advantage over the algebraic and geometric patch methods.

6. Conclusions

In this paper, we proved that the algebraic patch method is equivalent to an overlapping Schwarz method with subdomains enlarged by the patch regions. As a consequence,

Table 5. Same as in Table 4, but now with Krylov acceleration.

Mesh size h	Patch size	Geometric	Algebraic	Robin
1/50	$2h$	9	10	4
1/100	$2h$	12	14	5
1/200	$2h$	16	18	5
1/400	$2h$	24	27	6
1/50	$2h$	9	10	4
1/100	$4h$	9	10	4
1/200	$8h$	9	10	4
1/400	$16h$	9	10	4

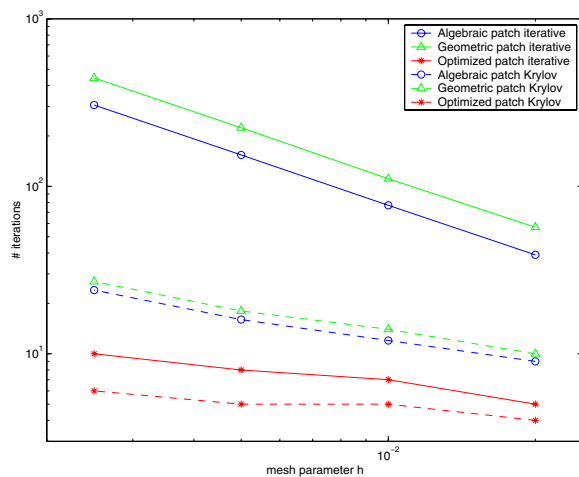


Fig. 6. Asymptotic comparison of the algebraic, geometric and optimized patch for a patch with the size proportional to the discretization parameter for a model problem.

the method converges independently of the mesh parameter, provided the patch size in physical space is kept constant. A similar result holds for the geometric patch substructuring method, which is also equivalent to an overlapping Schwarz method, albeit one that uses Neumann transmission conditions. A linear combination of the geometric and algebraic patch methods leads then to a new Robin patch substructuring method, and the parameter in the linear combination can be used to optimize the performance of the new method. We illustrated with numerical experiments that the Robin patch substructuring method is a very promising approach. We used the relation to optimized Schwarz methods to determine the optimal parameter in the Robin patch method, but it would be very desirable to have an algebraic way to determine this parameter. Also partial patches are not covered by the present analysis, and need a future study.

References

Chevalier P. and Nataf F. (1998): *Symmetrized method with optimized second-order conditions for the Helmholtz equation*. Contemporary Mathematics, Vol. 218, pp. 400–407.

Gander M.J. (2006): *Optimized Schwarz methods*. SIAM Journal on Numerical Analysis, Vol. 44, No. 2, pp. 699–731.

Japhet C. (1998): *Optimized Krylov-Ventcell method. Application to convection-diffusion problems*. Proceedings of the 9th International Conference Domain Decomposition Methods, Bergen, Norway, pp. 382–389.

Le Tallec P. (1994): *Domain decomposition methods in computational mechanics*, In: Computational Mechanics Advances, (J. Tinsley Oden, Ed.). North-Holland, Amsterdam, Vol. 1, No. 2, pp. 121–220.

Lions P.-L. (1988): *On the Schwarz alternating method. I*. Proceedings of the 1st International Symposium Domain Decomposition Methods for Partial Differential Equations, Philadelphia, PA: SIAM, pp. 1–42.

Lions P.-L. (1990): *On the Schwarz alternating method. III: A variant for nonoverlapping subdomains*. Proceedings of the 3rd International Symposium Domain Decomposition Methods for Partial Differential Equations, Philadelphia, PA: SIAM, pp. 202–223.

Magoulès F., Iványi P. and Topping B.H.V. (2004a): *Non-overlapping Schwarz methods with optimized transmission conditions for the Helmholtz equation*. Computer Methods in Applied Mechanics and Engineering, Vol. 193, No. 45–47, pp. 4797–4818.

Magoulès F., Roux F.-X. and Salmon S. (2004b): *Optimal discrete transmission conditions for a non-overlapping domain decomposition method for the Helmholtz equation*. SIAM Journal on Scientific Computing, Vol. 25, No. 5, pp. 1497–1515.

Magoulès F., Roux F.-X. and Series L. (2005): *Algebraic way to derive absorbing boundary conditions for the Helmholtz equation*. Journal of Computational Acoustics, Vol. 13, No. 3, pp. 433–454.

Magoulès F., Roux F.-X. and Series L. (2006): *Algebraic approximation of Dirichlet-to-Neumann maps for the equations of linear elasticity*. Computer Methods in Applied Mechanics and Engineering, Vol. 195, No. 29–32, pp. 3742–3759.

Quarteroni A. and Valli A. (1999): *Domain Decomposition Methods for Partial Differential Equations*. Oxford: Oxford University Press.

Saad Y. (1996): *Iterative Methods for Linear Systems*. Boston: PWS Publishing.

Schwarz H. (1870): *Über einen Grenzübergang durch alternierendes Verfahren*. Vierteljahrsschrift der Naturforschenden Gesellschaft in Zürich, Vol. 15, pp. 272–286.

Smith B., Björstam P. and Gropp W. (1996): *Domain Decomposition: Parallel Multilevel Methods for Elliptic Partial Differential Equations*. Cambridge: Cambridge University Press.

Toselli A. and Widlund O.B. (2004): *Domain Decomposition Methods: Algorithms and Theory*. Berlin: Springer.